You might find this additional information useful...

This article cites 62 articles, 11 of which you can access free at:
http://jn.physiology.org/cgi/content/full/90/6/3750#BIBL

This article has been cited by 10 other HighWire hosted articles, the first 5 are:

Effective and Structural Connectivity in the Human Auditory Cortex
J. Upadhyay, A. Silver, T. A. Knaus, K. A. Lindgren, M. Ducros, D.-S. Kim and H. Tager-Flusberg
J. Neurosci., March 26, 2008; 28 (13): 3341-3349.
[Abstract] [Full Text] [PDF]

Functional imaging of the auditory processing applied to speech sounds
R. D Patterson and I. S Johnsrude
Phil Trans R Soc B, March 12, 2008; 363 (1493): 1023-1035.
[Abstract] [Full Text] [PDF]

Spectrotemporal Analysis of Evoked and Induced Electroencephalographic Responses in Primary Auditory Cortex (A1) of the Awake Monkey
M. Steinschneider, Y. I. Fishman and J. C. Arezzo
Cereb Cortex, March 1, 2008; 18 (3): 610-625.
[Abstract] [Full Text] [PDF]

Evidence of Functional Connectivity between Auditory Cortical Areas Revealed by Amplitude Modulation Sound Processing
M. Gueguin, R. Le Bouquin-Jeannes, G. Faucon, P. Chauvel and C. Liegeois-Chauvel
Cereb Cortex, February 1, 2007; 17 (2): 304-313.
[Abstract] [Full Text] [PDF]

Automatic and Intrinsic Auditory "What" and "Where" Processing in Humans Revealed by Electrical Neuroimaging
L. De Santis, S. Clarke and M. M. Murray
Cereb Cortex, January 1, 2007; 17 (1): 9-17.
[Abstract] [Full Text] [PDF]

Updated information and services including high-resolution figures, can be found at:
http://jn.physiology.org/cgi/content/full/90/6/3750

Additional material and information about *Journal of Neurophysiology* can be found at:
http://www.the-aps.org/publications/jn

This information is current as of August 14, 2009 .

Functional Connections Between Auditory Cortex on Heschl's Gyrus and on the Lateral Superior Temporal Gyrus in Humans

John F. Brugge,[1,2,3] Igor O. Volkov,[1] P. Charles Garell,[1] Richard A. Reale,[2,3] and Matthew A. Howard III[1]

[1]*Department of Neurosurgery, University of Iowa College of Medicine, Iowa City, Iowa 52242; and*
[2]*Department of Physiology and* [3]*Waisman Center, University of Wisconsin, Madison, Wisconsin 53705*

Brugge, John F., Igor O. Volkov, P. Charles Garell, Richard A. Reale, and Matthew A. Howard III. Functional connections between auditory cortex on Heschl's gyrus and on the lateral superior temporal gyrus in humans. *J Neurophysiol* 90: 3750–3763, 2003. First published September 10, 2003; 10.1152/jn.00500.2003. Functional connections between auditory fields on Heschl's gyrus (HG) and the acoustically responsive posterior lateral superior temporal gyrus (field PLST) were studied using electrical stimulation and recording methods in patients undergoing diagnosis and treatment of intractable epilepsy. Averaged auditory (click-train) evoked potentials were recorded from multicontact subdural recording arrays chronically implanted over the lateral surface of the superior temporal gyrus (STG) and from modified depth electrodes inserted into HG. Biphasic electrical pulses (bipolar, constant current, 0.2 ms) were delivered to HG sites while recording from the electrode array over acoustically responsive STG cortex. Stimulation of sites along the mediolateral extent of HG resulted in complex waveforms distributed over posterolateral STG. These areas overlapped each other and field PLST. For any given HG stimulus site, the morphology of the electrically evoked waveform varied across the STG map. A characteristic waveform was recorded at the site of maximal amplitude of response to stimulation of mesial HG [presumed primary auditory field (AI)]. Latency measurements suggest that the earliest evoked wave resulted from activation of connections within the cortex. Waveforms changed with changes in rate of electrical HG stimulation or with shifts in the HG stimulus site. Data suggest widespread convergence and divergence of input from HG to posterior STG. Evidence is presented for a reciprocal functional projection, from posterolateral STG to HG. Results indicate that in humans there is a processing stream from AI on mesial HG to an associational auditory field (PLST) on the lateral surface of the superior temporal gyrus.

INTRODUCTION

The human forebrain neural circuitry involved in processing complex sound, including speech, is poorly understood. Based largely on evidence from nonhuman primates it is posited that this circuitry involves a number of functionally interconnected fields on the superior temporal gyrus (STG). Prominent among these fields, and located deep on the superior temporal plane on the mesial aspect of Heschl's gyrus (HG), is the primary auditory field (AI). AI cortex and the cortex adjacent to it having similar cytoarchitectural features are referred to collectively as the "core" of the auditory cortex. Auditory core areas have been identified on the superior temporal plane in humans (Galaburda and Sanides 1980; Hackett et al. 2001; Morosan et al. 2001; Rivier and Clarke 1997; Wallace et al. 2000), although there is not full agreement on their number or locations. In monkey the core areas receive input from the major divisions of the medial geniculate body (MGB) (Burton and Jones 1976; Hackett et al. 1998b; Mesulam and Pandya 1973; Morel and Kaas 1992; Morel et al. 1993; Walker 1938), from homologous regions of the opposite hemisphere (Boyd et al. 1971; Cipolloni and Pandya 1985, 1989; Fitzpatrick and Imig 1980; Pandya et al. 1969, 1973) and from a "belt" of cortex that surrounds the core (Fitzpatrick and Imig 1980; Hackett et al. 1998a; Morel and Kaas 1992; Pandya et al. 1969; Seltzer and Pandya 1978). This surrounding cortical belt may consist of a number of fields identified on the basis of cellular architecture, connectivity, or electrophysiology (Galaburda and Pandya 1983; Hackett et al. 1998a; Imig et al. 1977; Merzenich and Brugge 1973; Morel et al. 1993; Pandya et al. 1969; Rauschecker et al. 1995, 1997). The auditory belt receives both medial geniculate and auditory core input (Burton and Jones 1976; Fitzpatrick and Imig 1980; Hackett et al. 1998a,b; Morel et al. 1993). The auditory core in human is also surrounded by a belt of cortex that is responsive to acoustic stimulation (Binder et al. 2000; Talavage et al. 2000; Wessinger et al. 2001) and made up of multiple fields each having distinct cytoarchitecture and location (Hackett et al. 2001; Rivier and Clarke 1997; Wallace et al. 2000).

As with core areas, the number and location of belt areas are not completely known, and homologies with monkey belt areas remain highly speculative. Lateral to the auditory belt in the macaque monkey, and extending onto the lateral surface of the STG, is an auditory "parabelt," which is also made up of several fields whose major thalamic inputs are the dorsal and medial divisions of the MGB, the suprageniculate nucleus, the nucleus limitans, and the medial pulvinar. The parabelt also receives input from its counterpart on the opposite hemisphere, from the adjacent auditory belt but sparse, if any, input from the belt (Hackett et al. 1998a, 1999). The parabelt in monkey is most closely associated in humans with the area 22 of Brodmann (1909), which includes much of the lateral surface of the STG. Cortex making up the lateral surface of the STG is activated widely by a variety of speech and nonspeech sounds (see Binder et al. 2000), and includes on its caudal aspect an

auditory field we refer to as posterior lateral superior temporal field (PLST; Howard et al. 2000). Whether any of the belt cortex identified cytoarchitectonically or the lateral STG cortex activated acoustically should be considered the equivalent of the monkey parabelt is yet to be determined. Nonetheless, the hierarchical arrangement of interconnected auditory fields described in the macaque monkey provides an anatomical framework for possible parallel processing of acoustic information transmitted to cortical fields over thalamic routes as well as for serial processing of information over cortico-cortical pathways (Kaas and Hackett 1998; Kaas et al. 1999; Rauschecker 1998; Rauschecker et al. 1997).

Results of recent imaging studies are consistent with a hierarchical auditory processing model for human cortex as well (Binder et al. 2000; Wessinger et al. 2001). Little is known, however, of the anatomical connections between human cortical auditory fields. The anatomical track-tracing methods that have been used so effectively in mapping auditory cortical connectivity in the living monkey brain cannot be used in humans. Anatomical studies of auditory cortical interconnections in postmortem human specimens using carbocyanine dyes have revealed the presence of both intrinsic (Galuske et al. 2000) and extrinsic (Galuske et al. 1999) cortico-cortical connections within the STG. These studies have been necessarily limited to relatively short pathways that are typically revealed by this approach. Further knowledge of auditory cortical connections in humans would provide unique and valuable insight into the comparative anatomy and physiology of temporal auditory cortex, and would bridge data obtained on auditory cortical organization across humans and nonhuman primates.

An alternative method of tracing neural pathways in the cortical auditory system involves focal electrical stimulation of one cortical site while systematically mapping the resultant evoked activity from distant sites (Ades 1949; Bignall 1969; Bignall and Imbert 1969; Bremer et al. 1954; Downman et al. 1960; Howard et al. 2000; Imbert et al. 1966; Liegeois-Chauvel et al. 1991). This approach, of course, provides no direct information on the cellular origins, anatomical trajectories, or terminal arborations associated with neural pathways. It does, however, give direct information in the living brain on the functional connectivity between the site of electrical stimulation and the site(s) of recording. We have adopted this method to study in human epilepsy-surgery patients the functional connections between cortical fields, and in this paper describe the results of a study of functional connectivity between auditory cortex on HG and an associational auditory field on the lateral surface of the STG.

In a previous study (Howard et al. 2000) we reported an area of cortex on the posterolateral STG that could be activated by a wide variety of simple and complex sounds. This posterior lateral superior temporal area, which we called PLST, was differentiated on functional grounds from core auditory cortex on mesial HG (see also Hall et al. 2002; Wessinger et al. 2001). In that same study we showed that bipolar electrical stimulation of HG activates a circumscribed area of the lateral surface of the STG that overlaps the acoustically defined area PLST. These preliminary data suggested that a functional connection exists between the auditory core and PLST. The data presented here represent the results of a systematic investigation of this possible connection. These results provide evidence for the presence of a cortico-cortical processing stream between what we interpret to be primary auditory cortex and what might be considered a higher-order associational auditory field on the posterolateral surface of the STG.

METHODS

Subjects

The 7 subjects in this study were patients undergoing intracranial electrophysiological evaluation for medically intractable epilepsy before resection surgery. Six subjects were studied while they were awake and sitting up in their hospital bed. In one case we were able to carry out the experiment only when the patient was under general anesthesia just before resection surgery. Pure-tone audiograms and speech discrimination scores obtained preoperatively all fell within the normal range. The patients ranged in age from 19 to 46 yr (median = 38 yr). Recordings from 6 subjects were obtained from depth and surface grid electrodes implanted in the right cerebral hemisphere, which preoperative WADA testing showed to be the nondominant hemisphere for speech. One patient had grid and depth electrodes implanted in the left hemisphere. WADA testing in this patient was inconclusive regarding hemispheric dominance for speech. This patient had also undergone invasive monitoring and anterior temporal lobe resection 10 yr earlier, but had persistent seizures after resection surgery. Invasive monitoring was used in these cases because noninvasive diagnostic methods failed to define adequately the location of the seizure focus. Decisions regarding electrode placement and recording duration were based on the clinical needs of the individual patient. Research recording did not interfere with the clinical EEG recording. Informed consent was obtained after the nature and possible consequences of the studies were explained to the patient. Patients did not incur additional risk by participating in these studies. Research protocols were approved by the University of Iowa Human Subjects Review Board.

Intracranial electrodes

With the dura mater reflected a multicontact surface recording array (Radionics, Burlington, MA) was positioned over the middle and posterior aspects of the lateral STG under direct visualization. In some cases the array extended on to the perisylvian parietal cortex dorsally, the middle temporal gyrus ventrally, or both. Surface arrays consisted of platinum–iridium disc electrodes embedded in a silicon membrane. The center-to-center spacing of the electrodes on a grid was either 4 or 5 mm. The electrode contact diameter was 1.5 mm. Five subjects were implanted with an 8×8 array; the 2 others received a 12×5 array. Strip electrodes with 1-cm intercontact spacing were placed on the mesial surface of the inferior temporal gyrus and in 6 experiments served as reference leads for the differential recording of evoked potentials. In later experiments the reference electrode was attached to the skull near the midline in contact with the galia. In some cases a clinical grid with interelectrode spacing of 1 cm was also implanted more anteriorly on the lateral STG. We did not systematically record from these grid contacts for experimental purposes. A modified depth electrode [hybrid depth electrode (HDE); Howard et al. 1996b], was stereotactically implanted roughly parallel to the long axis of HG. Typically, this electrode carried 4 low impedance contacts (about 5 KΩ measured in situ) and as many as 20 higher impedance recording sites (0.08–0.2 MΩ measured in situ) distributed over its length. The distance between the first and last recording contacts was 3.5 cm.

Detailed intraoperative photographs, postimplantation X-rays, and pre- and postimplantation 3-dimensional (3D) MRIs were used together in localizing the grid and depth electrode recording sites. The 3D reconstruction was performed on the brain of each patient based on preoperative thin, contiguous MR images using Brainvox (Damasio and Frank 1992; Frank et al. 1997). Further details of the

surface grid array and the hybrid depth electrode and their methods of implantation can be found elsewhere (Howard et al. 1996a,b, 2000). In the experiments described here electrodes remained in place for periods ranging from 7 to 14 days (median = 10 days). In cases where there was more than one transverse gyrus, the depth electrode always traversed the anterior of these, reaching its mesial portion, which is the presumptive site of primary auditory cortex (Galaburda and Sanides 1980; Hackett et al. 2001; Morosan et al. 2002; Rademacher et al. 1993).

Acoustic stimulation and evoked potential recordings

Acoustic stimuli consisted of click trains presented every 2 s through insert earphones (Etymotic Research, Elk Grove Village, IL). All of these stimuli were effective in evoking high-amplitude stable potentials within HG and on the posterior aspect of the STG. Stimuli were delivered at a suprathreshold level that was comfortable for each patient. This was typically 50 dB above the detection threshold for the click-train stimulus. Threshold was estimated against the background sounds in the patient's hospital room. A slight variation (50 ms) in the interstimulus interval (ISI) reduced contributions of synchronous noise to the averaged evoked potentials (EP). Details of the acoustic response properties of HG and STG are beyond the scope of this study and will be presented elsewhere. For the purposes of this study, responses to click trains (5 clicks, 0.1-ms duration, 10-ms interclick interval) helped define the acoustically responsive regions of HG and posterior STG (Howard et al. 2000).

In 5 of the 7 subjects of this study EPs were recorded simultaneously from 8 or 12 electrodes on the surface array or the HDE. The EPs were amplified (Bak Electronics, Germantown, MD), filtered (band-pass 2–500 Hz), digitized (1 or 2 kHz sampling rate, DataWave, Longmont, CO), displayed on-line, and stored for off-line analysis. This was repeated until all electrodes on the array were sampled. Later in the series we introduced a new data acquisition system (Hewlett Packard E1432A Digitizer plus DSP) that permitted us to record simultaneously from 64 electrodes. This was used on 2 of the subjects in this study. We recorded EPs from the surface grid sites and from both the low- and high-impedance recording sites on the HDE. Acoustic evoked potentials shown in this study are the result of averaging 100 stimulus trials. Negativity is plotted upward in all figures.

Electrical stimulation

Once the location and approximate boundaries of PLST were determined using click-train stimulation, we initiated electrical-stimulation mapping experiments. An electrical stimulus was applied in bipolar fashion to adjacent acoustically active HG cortical sites while recording from cortex beneath the surface grid on the STG. This was repeated systematically for different HG sites. This provided us with information about the waveforms evoked by stimulation of different HG sites as well as maps of the spatial distribution of the functional projection of the stimulated HG sites to the STG. In 3 cases for which a HG-to-PLST functional projection was demonstrated we also studied the possible reciprocal projection by electrically stimulating acoustically active sites on the STG while recording from multiple sites along the HDE positioned within HG. This provided us with information regarding the spatial distribution of the functional projection to HG from the stimulated sites on the STG.

As a rule, a fast-rising rectangular pulse of depolarizing negative current is the most efficient waveform for extracellular stimulation, although extracellular anodal current can also stimulate axons (Yeomans 1990). In our experiments electrical stimuli were single 0.2-ms charge-balanced biphasic pulses applied in a bipolar fashion through a Grass SD9 stimulator. We are aware of the complexity of local activation patterns that such a bipolar stimulus configuration creates (see Brown et al. 1973; Rank 1975; Yeomans 1990) but using it proved necessary to minimize the stimulus artifact. Taking this into

consideration we use as a working assumption that the first negative pulse in the biphasic stimulus is the primary focus of cortical activation. Current strengths (estimated to be 1- to 4-mA peak) were maintained below after-discharge threshold (Ojemann and Engel 1986). Electrical stimuli were delivered at a rate of 1/s or 1/2 s, with the exception of experiments in which stimulus rate was the experimental variable. The averaged waveform from 50–100 stimulus trials was computed and displayed on-line, as described above for acoustic stimulation. Subjects reported no sensations resulting from electrical stimulation with these parameters. This is a safe procedure that has been used previously by us and others to study functional connections between temporal lobe regions in neurosurgical patients (Howard et al. 2000; Liegeois-Chauvel et al. 1991; Wilson et al. 1990).

RESULTS

Response fields on the posterior lateral superior temporal gyrus

Figure 1 illustrates for one subject the response maps obtained from acoustic (click) stimulation and from electrical stimulation of mesial HG, the presumed site of area AI. The location of the 64-channel recording grid is shown superimposed on a 3D MRI of this subject (*A*). To the right (*B*) is a horizontal MRI section showing a reconstruction of the bipolar stimulus sites in HG. Below are shown maps of averaged evoked potentials obtained by click-train stimulation (*C*) or by applying electrical stimuli to mesial HG sites (*D*) shown in *B*. We refer to the cortical area activated by sound or by electrical stimulation of a distant cortical site as a *response field*.

As a rule, robust evoked potentials to click stimulation were distributed over the posterior lateral aspect of the superior temporal gyrus, an area we refer to as *PLST*. The waveform of the polyphasic evoked potential varied across the response field, and it was not uncommon to see, as we do here, 2 foci of high-amplitude evoked potentials separated by a region in which the evoked potential was of lower amplitude. We have marked each of these 2 foci of maximal response with an asterisk on the map. In addition, the amplitude of the evoked response decreased with distance from the site(s) of maximal amplitude. Although we were always successful in recording from a region of maximal responsiveness, we were not always successful in determining the full extent of the response field because it often extended beyond the edges of the recording grid. These findings are typical of a large number of such experiments. Although it is beyond the scope of this study, we also note that area PLST responds robustly to a wide range of other acoustic stimuli including tones, noise, and speech sound. Although a clinical grid with more widely spaced contacts was sometimes placed more anteriorly on the STG, we do not have sufficient systematic data from this region to report at the present time.

Bipolar electrical stimulation of mesial HG activated an area of cortex that overlapped PLST (Fig. 1*D*). The evoked potential recorded at each site after HG electrical stimulation consisted of a series of positive and negative deflections occurring within about 50 ms of stimulus presentation. A stimulus artifact is clearly evident mainly on the left half of the grid, which tended to obscure possible early evoked activity at these sites. Like the acoustic response field, there was a cortical recording site where the evoked potential to electrical stimulation exhibited the greatest amplitude. This is also marked on the electrical response field by an asterisk. This site corresponds to one
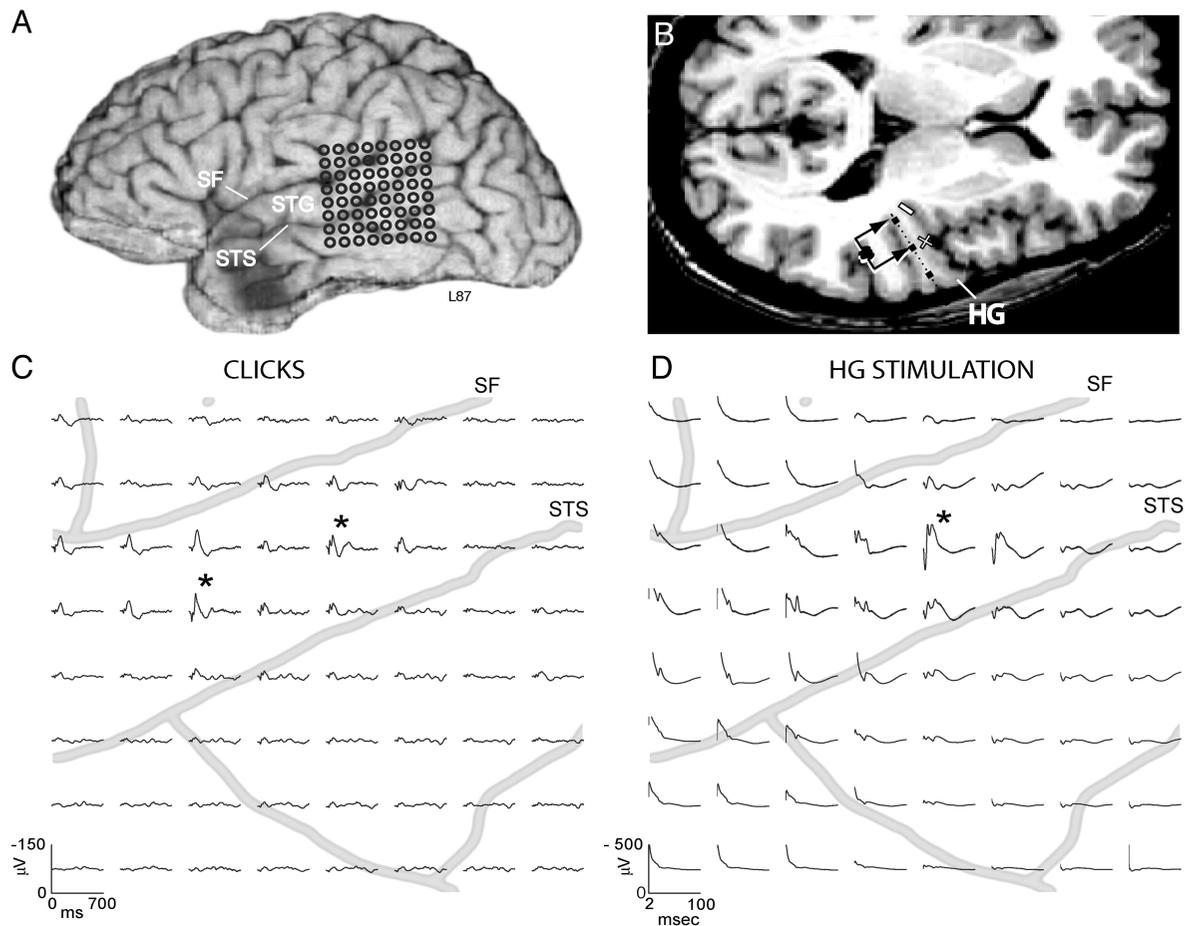
FIG. 1. Response fields on posterior superior temporal gyrus (STG). *A*: MRI showing location of recording grid on lateral surface of hemisphere. Grid overlays posterior aspect of superior temporal gyrus (STG) and extends above Sylvian fissure (SF) and below superior temporal sulcus (STS). *B*: horizontal MRI section at level of Heschl's gyrus (HG) showing trajectory of depth electrode and location of bipolar stimulation sites within HG. *C* and *D*: response fields on lateral STG resulting from click-train stimulation and electrical stimulation of mesial HG. Averaged evoked potentials derived from 100 repetitions of respective stimuli. In this and all subsequent figures negative voltage is up. Relative positions of recorded waveforms on maps of *C* and *D* represent relative positions of electrodes on recording grid shown in *A*. Gray lines represent locations of SF and STS. Asterisks mark sites of maximal response within 2 response fields.

of the 2 sites of maximal response within the acoustic response field.

Waveforms recorded on PLST to mesial HG stimulation

Figure 2 illustrates waveforms obtained at or near the site of maximal response amplitude within the electrical response field for each of the 6 subjects for which we have systematic data. The waveform complex in the 5 awake subjects is characterized by having an initial positive component followed by twin negative peaks (Fig. 2, *A–E*). The latency from stimulus onset to each peak in the waveform varied from one subject to the next. Peak latency of the earliest positive component varied from 3.2 to 6.0 ms. The earlier negative peak occurred 8.4–13.5 after stimulus onset, whereas the later negative peak had latencies ranging from 17.9 to 24.8 ms. The negative interpeak interval varied from 8.1 to 11.3 ms. Although waveforms having twin negative peaks tended to be most prominent at or near the site of maximal amplitude of response, systematic change in this waveform pattern could be seen across the map (e.g., Fig. 6). An exception to the rule of having waveforms

with twin negative peaks at the site of maximal amplitude was observed in one subject studied under general anesthesia (Fig. 2*F*). The waveform recorded at or near the site of maximal amplitude in this subject exhibited an initial positivity, but only a single, broad negative wave with a peak latency corresponding to the 2nd negative wave exhibited by the other 5 subjects.

On 2 occasions the stimulus artifact was very brief, and by using a high sampling rate we were able to capture the *onset time* of this early positive component (Fig. 3). Figure 3*A* shows for one of the subjects 4 superimposed evoked potentials recorded at and around the site of maximal amplitude. For the case illustrated in Fig. 3*B* only the evoked potential recorded at the site of maximal amplitude yielded a measurable onset latency. In each record a plateau was seen just after the stimulus artifact, which was then followed by a positive deflection. We estimated from these records that the onset of this 1st positive deflection occurred at 1.7 and 2.3 ms, respectively. Because in most instances the stimulus artifact obscured this very early activity evoked by mesial HG stimulation, we were unable to map systematically the spatial distribution of this early positive component, which we interpret to be the initial
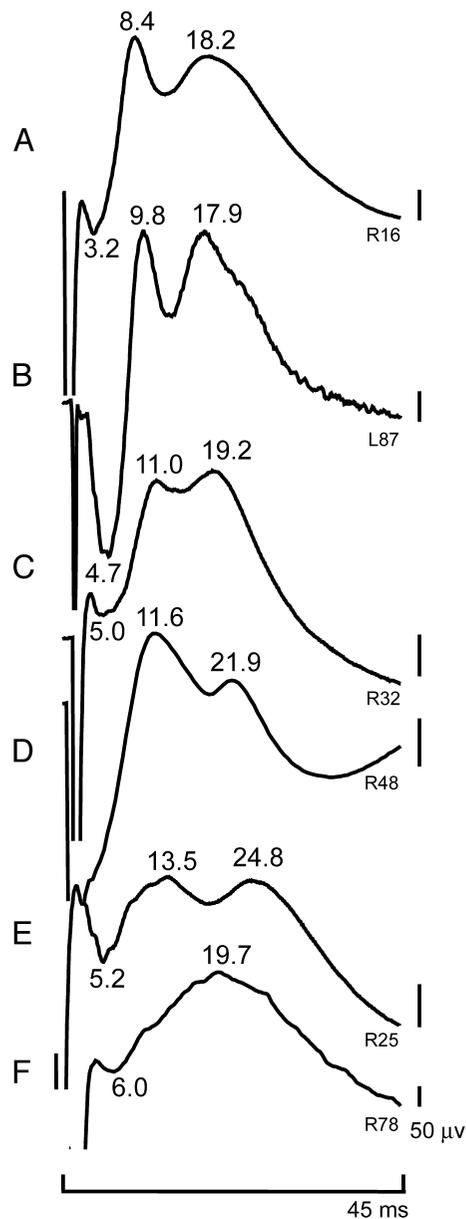
FIG. 2. Averaged waveforms recorded at site of maximal amplitude in 6 subjects in response to stimulus applied to mesial HG. Numbers represent peak latency (ms) measured from onset of stimulus. Early positive wave in *D* obscured by stimulus artifact. *A–E*: subjects awake. *F*: subject under deep surgical anesthesia. Vertical bar: 50 μV.

invasion of afferent input(s) to PLST activated by mesial HG stimulation.

Effects of varying interstimulus interval

The exact mechanisms by which electrical stimulation of HG cortex activates neural pathways functionally connected to lateral STG cortex are unknown. It seems likely, however, that the major peaks in the electrically evoked waveforms we recorded on lateral STG represent the sequential activation of intracortical circuitry within STG or of one or more afferent streams originating in mesial HG. We reasoned that if the peaks in the waveform represented activity in different intracortical circuits, activation of different converging pathways,

or both, they may exhibit different sensitivities to the rate of electrical stimulation. The results from 3 experiments, shown in Figs. 4 and 5, demonstrate this differential sensitivity.

The recording data shown in Fig. 4*A* were obtained after electrical stimulation of mesial HG from 8 electrodes arrayed linearly across PLST. The recording array included the site of maximal response (asterisk) in PLST. Figure 4*B* shows an expanded version of the evoked waveform recorded at the site of maximal response. At an ISI of 1,000 ms, which corresponds to the 1/s stimulus rate typically used in our mapping studies, the familiar early positive wave followed by twin negative peaks were evident at the site of maximum response (see also Fig. 2). Away from the site of maximal response in either direction along the array, the amplitude of the waveform diminished and the early positive component was obscured by the stimulus artifact. Reducing the ISI to 500 ms had little effect on the shape of the evoked potential at any of the 8 recording sites. When the ISI was reduced to 200 ms, however, a marked change in the waveform was observed. The early positive wave remained relatively unaffected, with a peak latency around 3.5 ms. However, the 1st of the successive negative peaks diminished in amplitude and lengthened in latency, whereas the amplitude of the 2nd negative peak was only marginally affected. A similar pattern was seen when the ISI was reduced even further, to 100 ms. The robustness of this finding is confirmed by data presented in Fig. 5 for 2 additional subjects. In these cases recordings are shown from 3 sites at and around the site of maximal response amplitude. At an ISI of 1,000 ms the early positive wave was seen along with the familiar twin negative peaks recorded at the site of maximal amplitude. In both cases little change was seen when the ISI was reduced from 1,000 to 500 ms. Reducing the ISI to 200 ms or less, however, had the same profound effect on the 1st of the
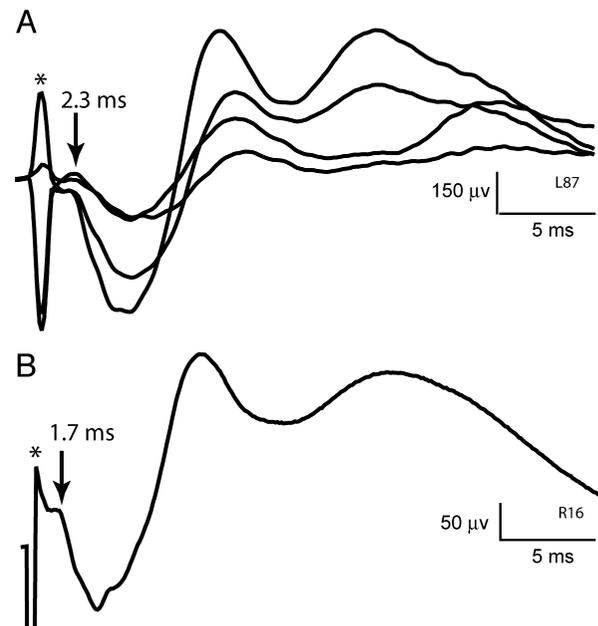

FIG. 3. Averaged waveforms recorded in posterior lateral superior temporal gyrus in 2 subjects in response to electrical stimulus applied to mesial HG. In these cases stimulus artifact (asterisk) did not obscure time of onset of early positive component (arrows). *A*: waveforms recorded at and around site of maximal amplitude of response. *B*: waveform recorded at site of maximal amplitude of response.

A

HG

1cm

ISI MSEC

*

1000

500

200

100

50μv
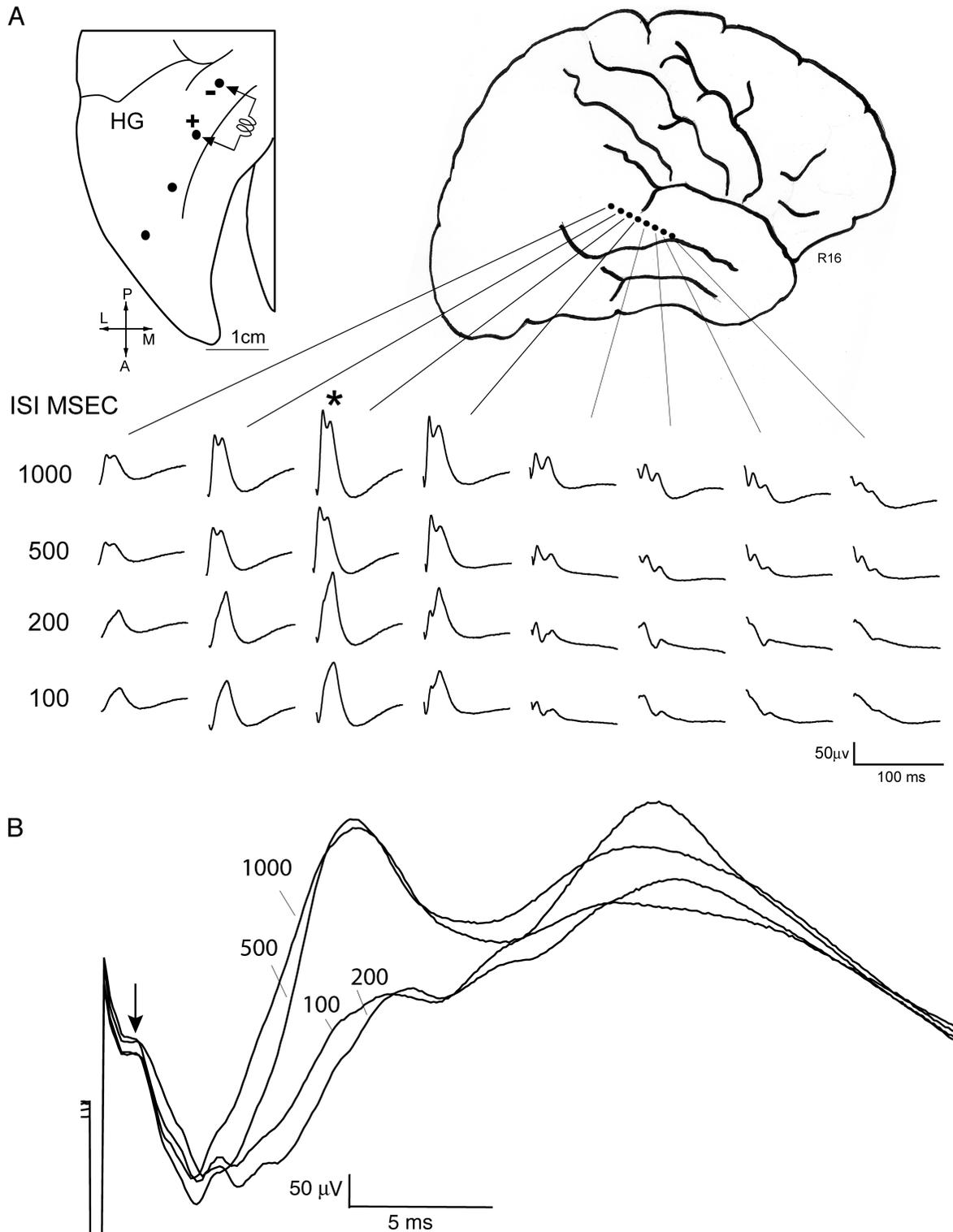100 ms

B

1000

500

200

100

50 μV
5 ms

FIG. 4. Effects of changing rate of electrical stimulation of mesial HG. *A*: outline drawings of the dorsal surface of the STG and lateral surface of the cerebral hemisphere obtained from MRIs. Sites of bipolar electrical stimulation on HG and recording on STG are shown on these outline drawings. Below are averaged waveforms recorded along a linear array of electrodes across STG in response to electrical stimulation of mesial HG. Each row obtained at a different rate of electrical stimulation, from 1 to 10/s. Interstimulus interval (ISI) shown to *left* of respective row of waveforms. Asterisk marks site of maximal amplitude of response. *B*: averaged waveforms recorded at site of maximal stimulation (asterisk) with time axis expanded to show details of waveform when stimulus rate was changed.
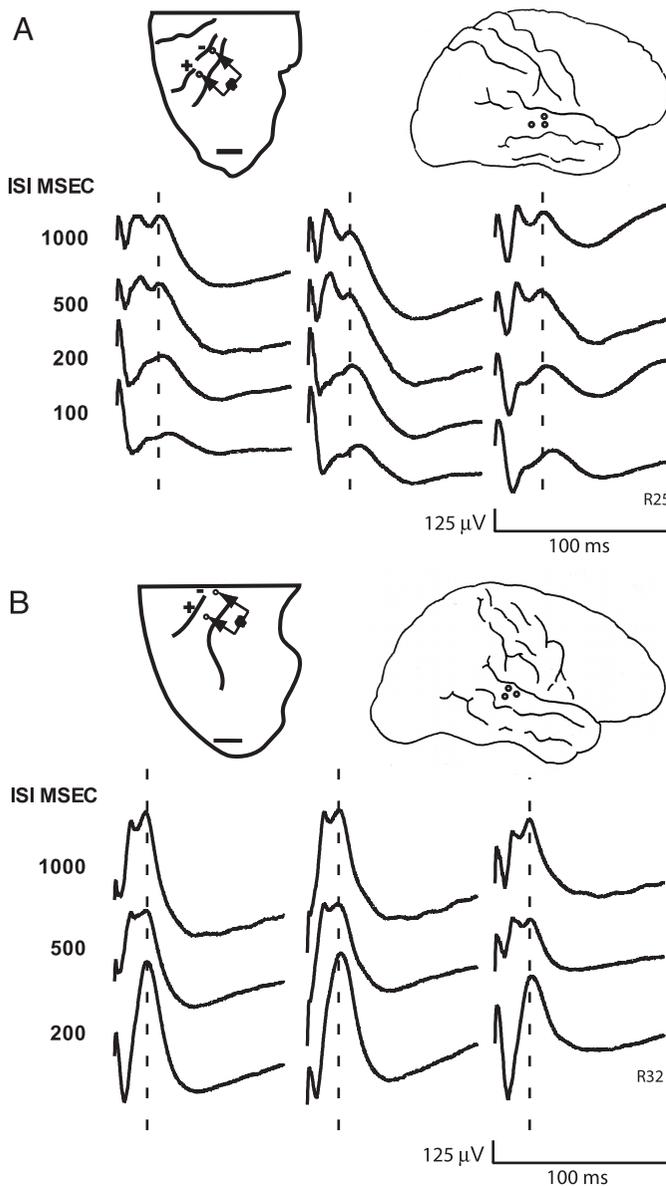
FIG. 5. Effects of changing rate of electrical stimulation of mesial HG. Averaged waveforms recorded at 3 sites within response field in 2 subjects in response to electrical stimulation of mesial HG. Location of stimulating and recording sites for each subject depicted on outline drawings of superior temporal plane and lateral surface of hemisphere, as in Fig. 4. For a time reference, dashed lines mark latency of second negative peak when ISI was 1 s.

2 peaks as seen in Fig. 4. The differential effect of changing stimulus rate on the response waveform suggests that these negative peaks arise from activation of different intracortical circuits, different afferent inputs, or some combination of the two.

The data presented so far provide evidence for a functional connection (or connections) between mesial HG, the putative site of AI in the auditory core, and an auditory association field on the lateral surface of the STG, area PLST. Histochemical cytoarchitectonic analyses (Wallace et al. 2000) and functional imaging (Binder et al. 2000; Wessinger et al. 2001) have suggested a belt field in humans occupying the lateral aspect of HG, adjacent to AI. We hypothesized that if these were 2 distinct fields then the functional connectivity between each of

them and PLST would differ. We could test this hypothesis given that the contacts positioned along the shaft of our depth electrode spanned the distance between mesial HG and the pial surface, thereby allowing us to systematically stimulate successive sites in presumed AI and in the adjacent lateral cortex on HG while recording from the even more lateral PLST.

Effects of varying site of HG stimulation

We were able to stimulate in 3 cases successively more lateral sites along the depth electrode while recording from the STG electrode array. Figures 6 and 7 illustrate results of these experiments. Data shown in Fig. 6 were recorded in the same subject and along the same linear electrode array as illustrated in Fig. 4. Each row of waveforms represents the response recorded from the same 8-electrode recording array but to stimulation of a different HG site. In each figure the stimulus sites having an initial negative polarity are shown to the left, on the schematic drawing of the superior temporal plane. The bipolar stimulus configuration is given to the left of each row of evoked potentials. The waveforms shown in the top row were the result of stimulation of the most mesial HG sites. These waveforms shown in Fig. 6 are comparable to those presented in Fig. 4, which were obtained from the same subject but at a different times during the experiment. Each evoked potential in this row is characterized by an early positive wave followed by 2 major negative peaks. The negative peak latencies (shown above the respective peak) and amplitudes varied systematically in a rostrocaudal direction across the array. The expanded waveforms shown at the bottom of Fig. 6 were obtained at 2 adjacent electrode sites on the recording array.

With electrical stimulation of successively more lateral HG sites the response field on the posterior STG remained in evidence, although the shape of the evoked waveform within it changed demonstrably. First, at any given recording site the latency of the peaks shortened systematically with successively lateral shifts of HG stimulation site. The latency changes, although systematic, were relatively small. At the site of maximal amplitude, for instance, there was an average difference of only 1.2 ms (from 9.4 to 8.2 ms) in latency to the earliest negative peak between the most mesial and most lateral stimulation sites. Second, as the HG stimulus site was shifted successively to more lateral locations the amplitude of the 2nd negative peak in the evoked waveform became progressively smaller, until with the most lateral stimulation it was hardly in evidence. The rather abrupt reduction or disappearance of the 2nd negative peak in the waveform between stimulus sites B and C suggests that a functional boundary exists between auditory cortex on mesial HG and cortex located more laterally on HG on the supratemporal plane.

The robustness of this finding, along with an additional observation, are shown in Fig. 7 for another subject. In this case, the 8 STG recording sites include the site of maximal response (asterisk). At this site, and at several sites rostral to it, we observe the familiar twin negative peaks resulting from mesial HG stimulation (Stim A). These peaks are marked with dashed lines. Stimulation of a lateral site on HG (Stim B) resulted in waveforms in which the 1st peak, when present, appeared earlier and severely attenuated, and the 2nd peak was not evident. At several sites an early positive wave was re-
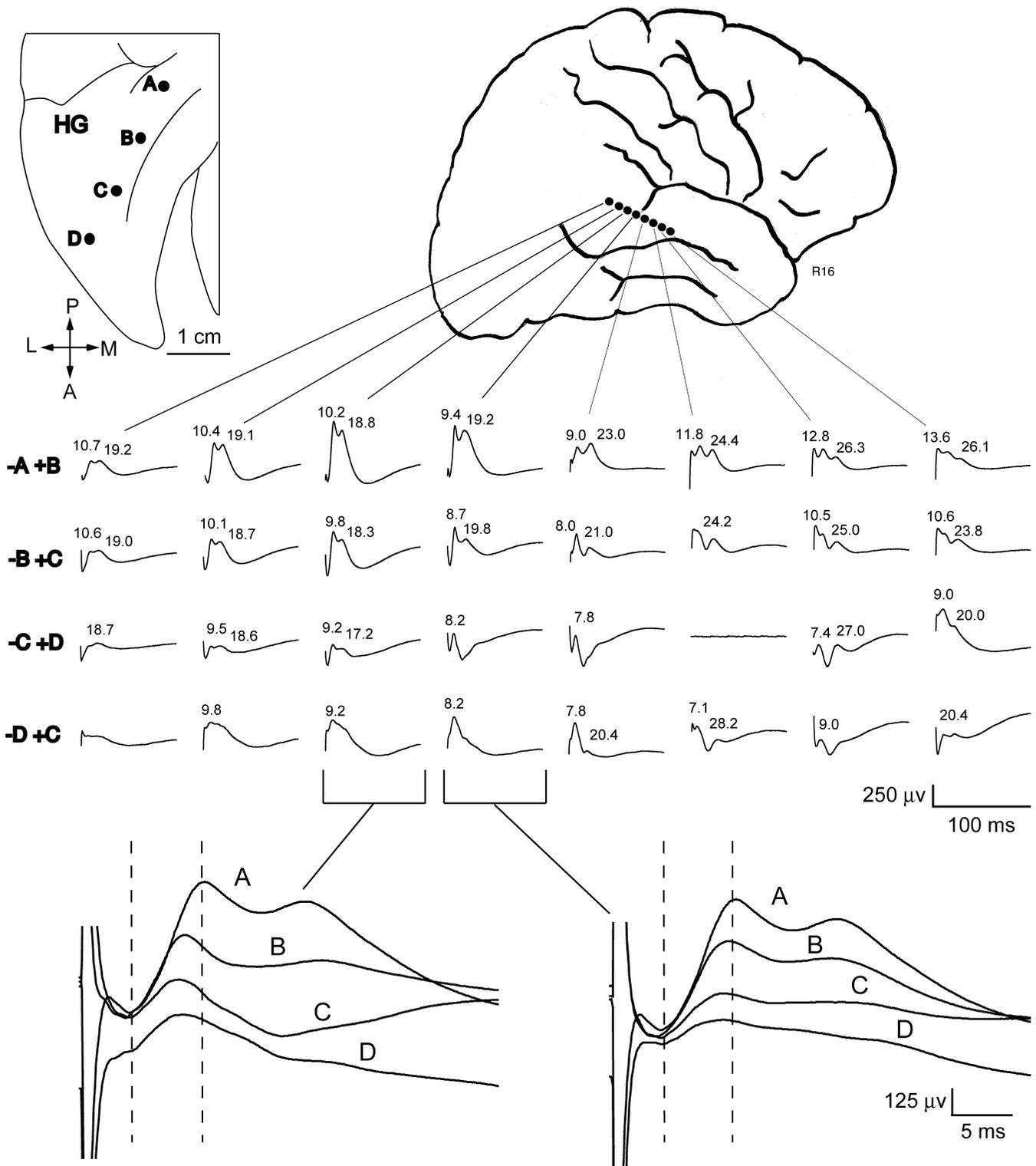
FIG. 6. Effects of successively changing HG stimulus site on averaged waveforms recorded along a linear array of electrodes through response field on STG. Each row obtained at a different HG stimulus site. Bipolar stimulation sites on HG and location of recording array shown above. Peak latency (ms) indicated above respective peaks. Below are averaged waveforms recorded at or near site of maximal response amplitude with time axis expanded to show details of waveform when stimulus site was changed. Dashed lines mark latency of early positive peak and first negative peak when stimulation was applied to most mesial site on HG. Stimulus site designated on each waveform.
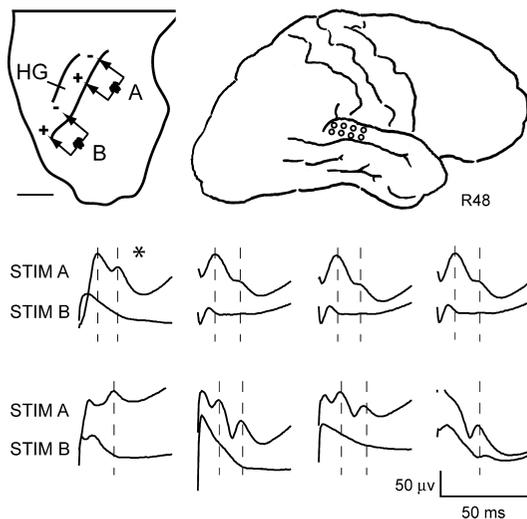
FIG. 7. Effects of changing stimulus site on HG. Averaged waveforms recorded at 8 recording sites at and around site of maximal amplitude in response to stimulating mesial (*A*) and lateral (*B*) sites on HG. Asterisks mark site of maximal amplitude of response. Dashed lines mark latency of negative peaks obtained when stimulus was applied to mesial HG.

corded and it remained relatively unchanged, whereas the later negative waves were nearly abolished.

Summarizing these results it appears that both negative peaks in the evoked waveform arise from activating a cortico-cortical pathway, or pathways, originating in mesial HG. The more lateral HG cortex apparently contributes little to the 2nd major negative peak, given that this peak is essentially absent after stimulation of lateral HG sites. The 1st negative peak is present regardless of the stimulus site. Its systematic decrease in latency with decreasing distance between stimulation and recording sites may suggest that we were stimulating axons of passage that originate in mesial HG and run within the white matter beneath the stimulating electrode.

Effects of stimulation of PLST on activity recorded from HG

Auditory cortical fields in monkey have been shown to exhibit reciprocal connections (Hackett et al. 1998b). Having shown that HG sends a functional projection to PLST we carried out the reverse experiment by stimulating electrically sites within PLST while recording the response evoked by that stimulus at various sites along the depth electrode in HG. The PLST sites chosen were at or near the site of maximal amplitude response to HG stimulation. We observed robust evoked responses from sites along the mediolateral axis of HG in all 3 cases studied this way. The major findings, which were consistent across subjects, are illustrated in Fig. 8.

Figure 8*A* shows 8 waveforms recorded from 8 high-impedance and low impedance contacts distributed along HG. For the 5 electrode recording sites in mesial HG, a major positive peak occurred some 25–30 ms after electrical stimulation followed by a large negativity around 60–70 ms. This positive–negative complex was in some cases preceded by a smaller negative peak at about 12 ms. The overall amplitude of this waveform complex increased mediolaterally until a transition zone was reached within which the waveform altered its shape and diminished substantially in amplitude. An arrow marks the site of this transition. A similar family of waveforms is shown for

another subject in Fig. 8*B*. Here data were obtained only from low-impedance contacts. Again there is a transition in the waveform shape and amplitude around the middle of HG, and again it is marked with an arrow. The third example (Fig. 8*C*), derived from recordings from both high-impedance and low-impedance contacts, shows that in this subject little activity was evoked at the most mesial recording site. The first sign of an evoked potential appears at the adjacent recording site, and the EP reaches its maximal amplitude toward the middle of HG. A transition then took place (arrow) as the amplitude and shape of the evoked response at the more lateral recording sites changed markedly. The results of these 3 experiments taken together indicate that area PLST projects functionally, though differentially, over most, if not all, of the length of HG. Furthermore, we take the transition in the shape of the evoked waveform that occurs along HG as marking a functional boundary between auditory cortex on mesial HG and an auditory belt situated more laterally on HG.

As described earlier, changing the rate of electrical stimulation to HG had a profound, but differential, effect on the several peaks in the evoked waveform complex recorded in PLST. We now show in Fig. 9 that under the reverse situation changing the rate of PLST electrical stimulation had only a small but demonstrable effect on the evoked response in HG. In this figure data from the 4 HG recording sites illustrated in Fig. 8*B* are shown at 4 ISIs. Dashed lines mark the peaks of the early and late negative peaks when the ISI was 1,000 ms. Reducing the ISI resulted in a small but systematic shift in the amplitude of both peaks, a broadening of the positive component, and a slight lengthening of the later negativity.

DISCUSSION

Electrical stimulation of HG resulted in polyphasic evoked activity on posterolateral STG within 50 ms of stimulus onset. Electrically induced evoked potentials were found within a circumscribed area (a response field) that overlapped a region on the posterolateral aspect of the STG activated by acoustic stimulation, a region we refer to as area PLST (see Howard et al. 2000). The most robust and complex waveform resulted from stimulation of sites within about the mesial 1/2 of HG, the presumed site of AI in humans. These results provide prima facie evidence for a functional projection from auditory cortex on HG to an associational auditory cortex (PLST) on the lateral surface of the STG in human.

The earliest studies of functional connectivity of auditory cortex, in the anesthetized rhesus monkey (Sugar et al. 1948; Ward et al. 1946) and chimpanzee (Bailey et al. 1943), were carried out using the method of strychnine neuronography. In both species local application of strychnine to primary auditory cortex resulted in spikes being propagated to area 22 on the lateral surface of the STG. Whereas this approach gave evidence for a functional connection between presumed AI and a field on the lateral STG, it provided no information on the timing or magnitude of the projection or on the spatial relationship between it and any acoustically responsive region. Later, Bignall (1969) showed that electrical stimulation of presumed AI in the anesthetized squirrel monkey elicited a large positive-going evoked potential on the convexity of STG and suggested that this response may have been recorded from the homolog of area 22 in the macaque monkey, although no
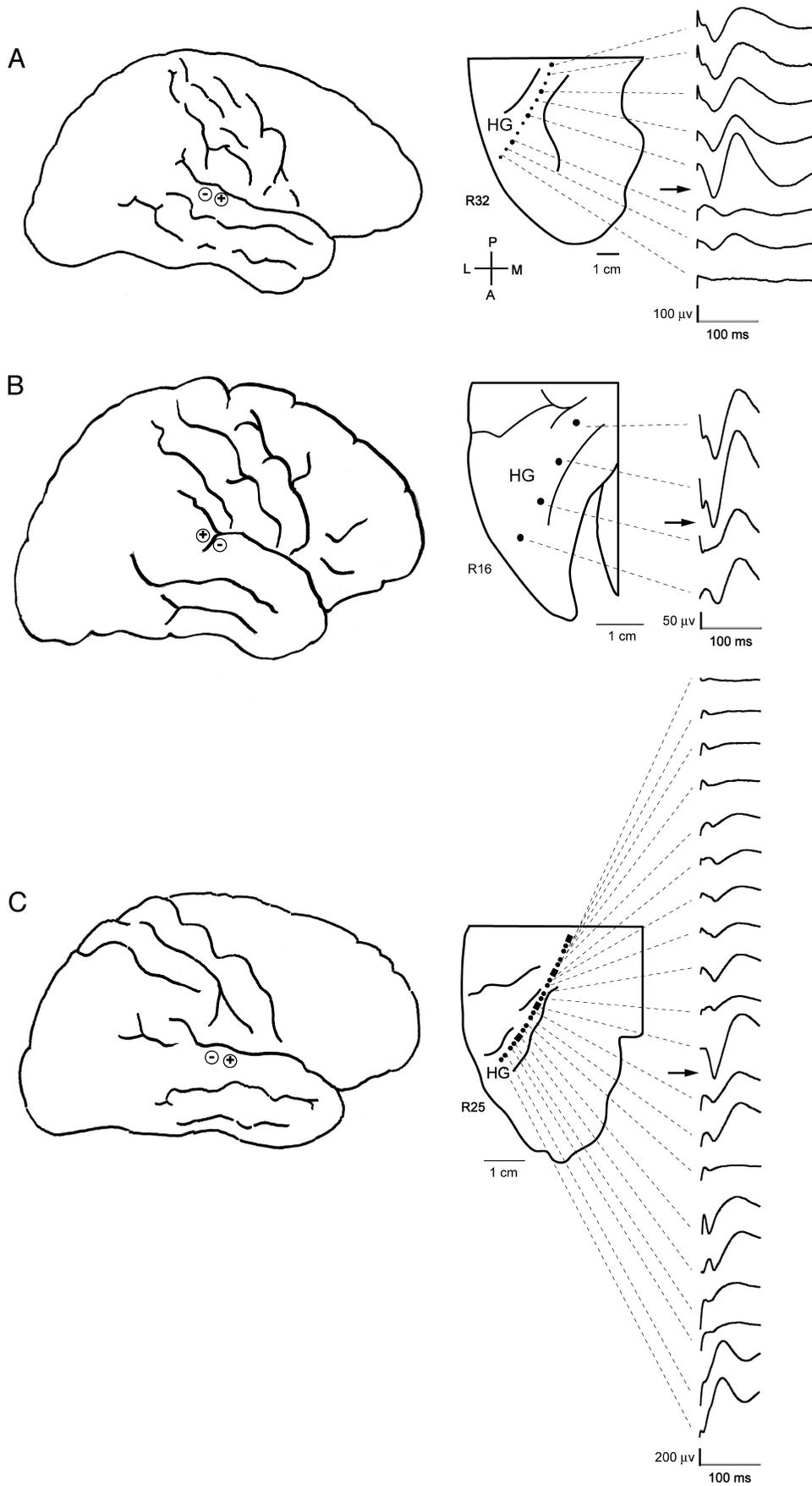
FIG. 8. Waveforms evoked along HG by bipolar electrical stimulation of most active site on PLST. Location and polarity of bipolar stimulation shown. Arrows point to site along HG where evoked waveform changed abruptly. Small circles: high-impedance contacts; large circles: low-impedance sites.
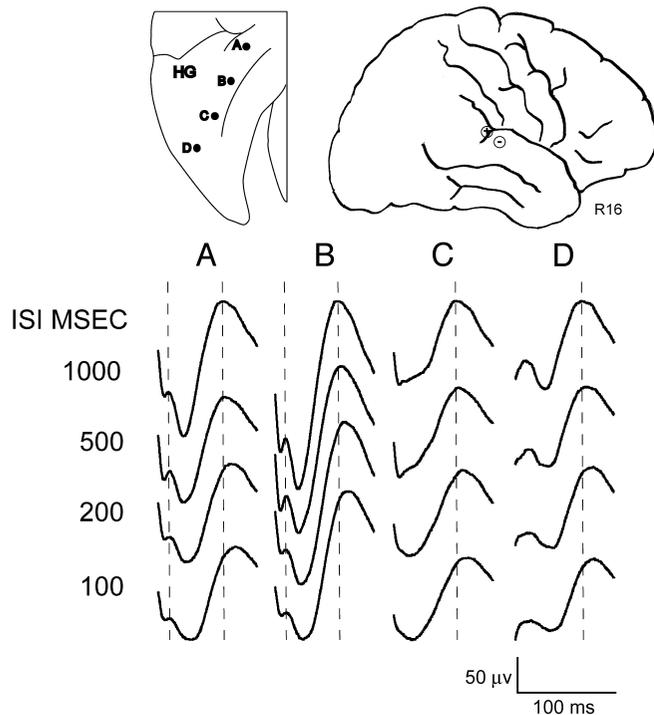
FIG. 9. Waveforms evoked at sites along HG at different rates of bipolar electrical stimulation of most active sites in area PLST. For a time reference, dashed lines mark latency of major negative peaks in waveform at an ISI of 1 s.

histological verification was reported. We now know that primary auditory cortex in the squirrel monkey (Woolsey 1971) and in its new-world relative the owl monkey (Imig et al. 1977; Morel and Kaas 1992; Woolsey 1971), probably extends onto the lateral surface of the STG, and hence these electrical stimulation results may instead provide evidence for intrinsic AI connectivity or for an AI projection to an adjacent field. Liegeois-Chauvel et al. (1991) reported the first evidence for a functional connection between auditory cortical fields in the human. They found that electrical stimulation of mesial HG in human evoked activity on laterally adjacent HG cortex as well as on the planum temporale. These are areas that subsequently have been identified both anatomically and functionally as part of an auditory belt (Rivier and Clarke 1997; Talavage et al. 2000; Wallace et al. 2000; Wessinger et al. 2001) that surrounds an auditory core (Hackett et al. 2000).

We showed that a waveform complex composed of an initial positive deflection followed by one or more negative waves was typically recorded on the posterior lateral STG in response to electrical stimulation of presumed AI. The shape of the evoked waveform, including the magnitude, number, and latency of the peaks, depended on the recording site on STG. At or near the site of maximal responsiveness in PLST the waveform was characterized by an early positive wave followed by twin negative peaks. It is generally accepted that the waveform recorded by an electrode on the brain surface varies in magnitude and polarity over time depending on the timing, strength, and location of synaptic current sinks and sources (see Arezzo et al. 1986; Mitzdorf 1985, 1991, 1994; Mitzdorf and Singer 1978; Vaughan and Arezzo 1988). We interpret the positive and negative events in our recorded waveforms after a stimulus, whether it be acoustic or electrical, as reflecting the summation of ionic current flowing mainly within the cortex

immediately beneath the recording electrode, created by the invasion of stimulus-evoked input arriving over one or more afferent pathways. Although evoked potentials reflect mainly synaptic events, a very early presynaptic afferent volley may appear as a small negativity. This component, if present in our records, would probably have been obscured by the stimulus artifact.

The earliest waveform component we detected with any consistency evoked by mesial HG stimulation was a surface positive wave having an average onset latency of about 2 ms and an average peak latency ranging across subjects from about 3 to 6 ms. We interpret this early positive component as representing a deep sink with a superficial source created by the 1st invading afferent volley evoked by mesial HG stimulation. This interpretation is consistent with what is known of auditory cortico-cortical projections to layers III and IV in owl monkey (Fitzpatrick and Imig 1980) and with current source density profiles of auditory cortex in rhesus monkey (Steinschneider et al. 1982). We may speculate that the later negative peaks represent shallow cortical depolarizations within supragranular layers. It is possible also that the trough between the major negative peaks represents a superficial current source. Although we have no systematic data to present on the effects of general anesthesia, we did observe in one subject that under these conditions the early positive component was in evidence followed by a single late negative wave having a latency within the range of later negative waves recorded in awake subjects. These results would suggest that the 2 negative waves arise over separate circuits, differentially sensitive to anesthesia, that converge on PLST. If this is the case then the proposed convergent input is segregated *temporally*, as the differences in peak latency would imply. Whether there is *spatial* segregation as well is something that is yet to be determined.

The question arises concerning the neuronal pathway(s) activated by mesial HG stimulation that eventually terminate in and activate, in turn, area PLST. Based on findings in monkey there are several possible candidates including cortico-cortical pathways within the ipsilateral cortex (Hackett et al. 1998a), pathways that cross to the opposite cerebral hemisphere (Fitzpatrick and Imig 1980; Hackett et al. 1999; Morel and Kaas 1992; Morel et al. 1993; Pandya et al. 1973), and pathways that connect cortical fields by way of the thalamus (Hackett et al. 1998b; Morel and Kaas 1992; Morel et al. 1993; Pandya et al. 1994). From latency measurements of the major peaks in the waveform complex, and making certain assumptions about the caliber and conduction velocity of cortico-cortical axons, we may infer possible pathways that originate in mesial HG cortex and eventually converge on PLST.

Considering onset latencies of about 2 ms it is not likely that the earliest positive wave we recorded was the result of activating an interhemispheric pathway or a cortico-thalamo-cortical loop. Kitzes and Doherty (1994) found that in ferret the average 1st spike latency recorded from an AI neuron to electrical stimulation of contralateral AI ranged from about 2 to 14 ms (mean 5.4 ms). These values are consistent with results obtained by Mitani and Shimokouchi (1985) in their study of excitatory postsynaptic potentials recorded in cat auditory cortex evoked by contralateral electrical stimulation. Latency recorded in MGB or inferior colliculus to auditory cortical stimulation (Mitani et al. 1983) would also seem to rule out pathways involving these structures as contributing to the early

positive wave in the response particularly if one adjusts for substantially longer transmission pathways in the human brain as compared with those of laboratory animals in which they have been described.

We estimate from MRI data that the distance from the stimulating electrode on mesial HG to the STG recording sites was about 4–5 cm. Bishop and Smith (1964) estimated the average diameter of axons of the white mater of the human frontal lobe to be between 0.8 and 1.5 microns, with a very small proportion of axons lying outside of this range. We have no direct knowledge of the diameter of cortico-cortical axons that might connect mesial HG with the posterior lateral STG. If, however, we assume a similar spectrum of fiber diameter reported in human frontal lobe, and using the relationship of conduction velocity to axonal diameter for central axons derived by Waxman and Swadlow (1977), we predict that for axons of 0.8–1.5 microns and lengths of 4.0–5.0 cm the expected average peak latency would be between about 4.5 and 12 ms. If we include in our estimate fibers of greater diameter within the frontal lobe fiber spectrum it would not be surprising to see onset latencies around 2 ms. These estimates derived from axonal conduction times in cortical white mater are in good agreement with our measured estimates of the latencies of the onset (2 ms) and peak (3–6 ms) of the earliest positive evoked component, which we interpret as the 1st afferent input to middle cortical layers. From these considerations we may conclude that in humans an ipsilateral cortico-cortical projection exists from mesial HG cortex to PLST. These estimates of transmission time are compatible with an indirect cortico-cortical connection with a possible intervening synaptic delay in adjacent belt field. They do not, however, exclude the possibility that a component of this functional projection may reflect a direct connection. This latter suggestion is given further credence by our finding that stimulation of the more lateral sites on HG resulted in loss of the 1st negative component recorded at or near the site of maximal response in PLST. Indeed, it was surprising to us that the activity evoked by lateral HG stimulation was so ineffective in evoking activity in PLST.

Interpreting the sources of input that result in the later negative peaks is even less straightforward. Our finding that changing the rate of electrical stimulation of mesial HG reduced selectively the 1st of the negative peaks in the waveform suggests that the 2 negative peaks either arise from activation of 2 different pathways or they represent 2 different intracortical circuits. The latency of the earliest of the negative peaks (8.4–13.5 ms) could be accounted for by input arriving over the smallest diameter cortico-cortical axons with or without intervening synaptic delay and ending in superficial cortical layers where they would create a superficial current sink. Alternatively, both peaks could be accounted for by later-arriving afferent input arriving over longer interhemispheric or cortico-thalamo-cortical pathways that are likely activated by mesial HG stimulation.

We presented evidence consistent with the hypothesis that in humans an auditory belt field intervenes between core cortex on mesial HG and the more lateral area PLST. This comes from our observation that waveforms recorded from PLST change with stimulus location along the HG. When the electrical stimulus was applied to mesial HG the waveform consisted of an early positive wave followed by twin negative

peaks. The 2nd negative peak was severely attenuated or disappeared when the stimulus was applied to more laterally positioned sites along the HG. We conclude from this that both negative peaks represent afferent input originating from mesial HG. The single negative peak evoked in isolation from more lateral HG stimulation may be interpreted as arising from a lateral auditory belt field on the superior temporal plane. Alternatively, we cannot rule out the possibility that it could have arisen by stimulation of cortico-cortical axons originating mesially and coursing beneath the stimulating electrode. This latter suggestion is consistent with our observation of a small, but systematic decrease in peak latency when the electrical stimulus was applied more laterally along HG.

Galuske et al. (1999) carried out anatomical tracer studies in postmortem specimens of human auditory cortex showing that there are reciprocal connections between Brodmann area 41 (primary auditory cortex) and areas 42 laterally and 51 rostrally and that area 42 makes reciprocal connections with anterior, but not posterior, area 22. These findings could be interpreted as being consistent with those in rhesus monkey (Hackett et al. 1998a). They may also help explain our finding of a more robust response to simulation of mesial than of lateral HG. If the HG cortex lateral to presumed AI projects preferentially to more anterior sites on STG we may not have seen it because we often did not have grids in that location and even when we did, we focused the experiments on the posterior recording sites. If this turns out to be the case, then the robust PLST response to stimulation of mesial HG may be either the result of a direct projection from AI to PLST or an indirect one with synaptic interruption in a belt area that we did not stimulate. In macaque monkey posterior belt cortex projects preferentially to posterior parabelt cortex (Hackett et al. 1998a). If the same holds true in humans then one of the posterior belt fields identified histochemically by Rivier and Clarke (1997) and Wallace et al. (2000)—perhaps their field LA on the planum temporale— would be a candidate for such an intermediate synaptic station. Further evidence to support this idea comes from the studies of Liegeois-Chauvel et al. (1991) showing that electrical stimulation of mesial HG evokes a response on the planum temporale. The onset latency varied from 6 to 8 ms and the peak latency from 10 to 20 ms. This event occurs later than the earliest positive peak in the PLST response, and may even exceed slightly the timing of the 1st negative component. However, it appears slightly earlier than the 2nd negative peak in the PLST waveform, which is what would be expected if this area on the planum temporale is to be considered a synaptic relay between AI and PLST. We might speculate further that a distinct area situated lateral to LA—referred to as area STA by Rivier and Clarke (1997)—may correspond, at least in part, to our area PLST. Further functional studies that include more of the supratemporal plane and the lateral STG are under way to clarify where PLST is to be placed in a serial processing stream emerging from the auditory core. This new information will also be critical in determining the extent to which the anatomical framework of organization derived from studies in monkey can be successfully applied to the human.

We found that stimulation of sites within the response field on posterior lateral STG evoked responses all along HG. These results are in accord with the early observations of Bailey et al. (1943) in chimpanzee and Sugar et al. (1948) in rhesus monkey that strychnization of area 22 causes spikes to appear in the

primary auditory cortex. Bignall (1969) on the other hand reported that electrical stimulation of lateral STG in squirrel monkey failed to evoke activity in presumed area AI. In the current study the waveforms evoked in HG by electrical stimulation of PLST were demonstrably different from those recorded when stimulus and recording sites were reversed. In mesial HG, the waveform was characterized by an early small negativity followed by a large positive wave having a peak latency around 20–25 ms. These latencies are compatible with finding in monkey of a polysynaptic pathway from PLST to mesial HG and of a paucity of connections from the lateral association area back to the primary auditory cortex (Hackett et al. 1998a; Pandya et al. 1969).

The evoked waveform recorded in HG was relatively resistant to changes in interstimulus interval, which suggests that the synaptic connections of this pathway differ from those in the HG-to-STG projection. Finally, there was an abrupt change in the waveform around the middle of HG. This may have signaled the presence of a transition zone between an auditory belt and presumed AI. These results taken together suggest that the pathways making up the PLST– HG projection are fundamentally different from those that underlie the HG–PLST circuits.

REFERENCES

Ades HW. Functional relationship between the middle and posterior ectosylvian areas in the cat. *Am J Physiol* 159: 561, 1949.

Arezzo JC, Vaughan HG Jr, Kraut MA, Steinschneider M, and Legatt AD. Intracranial generators of event related potentials in the monkey. In: *Evoked Potential Frontiers of Clinical Neuroscience*, edited by Cracco RQ and Bodis-Wollner I. New York: Alan R. Liss, 1986, p. 174–189.

Bailey P, Von Bonin G, Carol HW, and McCulloch WS. Functional organization of temporal lobe of monkey (*Maccaca mulatta*) and chimpanzee (*Pan satyrus*). *J Neurophysiol* 6: 121–128, 1943.

Bignall KE. Bilateral temporofrontal projections in the squirrel monkey: origin, distribution and pathways. *Brain Res* 13: 319–327, 1969.

Bignall KE and Imbert M. Polysensory and cortico-cortical projections to frontal lobe of squirrel and rhesus monkeys. *Electroencephalogr Clin Neurophysiol* 26: 206–215, 1969.

Binder JR, Frost JA, Hammeke TA, Bellgowan PS, Springer JA, Kaufman JN, and Possing ET. Human temporal lobe activation by speech and nonspeech sounds. *Cereb Cortex* 10: 512–528, 2000.

Bishop GH and Smith JM. The sizes of nerve fibers supplying cerebral cortex. *Exp Neurol* 9: 481–501, 1964.

Boyd EH, Pandya DN, and Bignall KE. Homotopic and nonhomotopic interhemispheric cortical projections in the squirrel monkey. *Exp Neurol* 32: 256–274, 1971.

Bremer F, Bonnet V, and Terzuolo C. Etude electrophysiologiaque des aires auditives corticales chez le chat. *Arch Int Physiol* 62: 390–428, 1954.

Brodmann K. *Vergleichende Lokalisationslehre der Grosshirnrinde.* Leipzig, Germany: J. A. Barth, 1909.

Brown PB, Smithline L, and Halpern B. Stimulation techniques. In: *Electronics for Neurobiologists*, edited by Brown PB, Maxfield BW, and Moraff H. Cambridge, MA: MIT Press, 1973.

Burton H and Jones EG. The posterior thalamic region and its cortical projection in new world and old world monkeys. *J Comp Neurol* 168: 249–302, 1976.

Cipolloni PB and Pandya DN. Topography and trajectories of commissural fibers of the superior temporal region in the rhesus monkey. *Exp Brain Res* 57: 381–389, 1985.

Cipolloni PB and Pandya DN. Connectional analysis of the ipsilateral and contralateral afferent neurons of the superior temporal region in the rhesus monkey. *J Comp Neurol* 281: 567–585, 1989.

Damasio H and Frank R. Three-dimensional in vivo mapping of brain lesions in humans. *Arch Neurol* 49: 137–143, 1992.

Downman CB, Woolsey CN, and Lende RA. Auditory areas I, II and Ep: cochlear representation, afferent paths and interconnections. *Bull Johns Hopkins Hosp* 106: 127–142, 1960.

Fitzpatrick KA and Imig TJ. Auditory cortico-cortical connections in the owl monkey. *J Comp Neurol* 192: 589–610, 1980.

Frank R, Damasio H, and Grabowski TJ. Brainvox: an interactive, multimodal visualization and analysis system for neuroanatomical imaging. *Neuroimage* 5: 13–30, 1997.

Galaburda AM and Pandya DN. The intrinsic architectonic and connectional organization of the superior temporal region of the rhesus monkey. *J Comp Neurol* 221: 169–184, 1983.

Galaburda AM and Sanides F. Cytoarchitectonic organization of the human auditory cortex. *J Comp Neurol* 190: 597–610, 1980.

Galuske RA, Schlote W, Bratzke H, and Singer W. Interhemispheric asymmetries of the modular structure in human temporal cortex. *Science* 289: 1946–1949, 2000.

Galuske RAW, Schuhmann A, Schlote W, Bratzke H, and Singer W. Interareal connections in the human auditory cortex. *Neuroimage* 9: S994, 1999.

Hackett TA, Preuss TM, and Kaas JH. Architectonic identification of the core region in auditory cortex of macaques, chimpanzees, and humans. *J Comp Neurol* 441: 197–222, 2001.

Hackett TA, Stepniewska I, and Kaas JH. Subdivisions of auditory cortex and ipsilateral cortical connections of the parabelt auditory cortex in macaque monkeys. *J Comp Neurol* 394: 475–495, 1998a.

Hackett TA, Stepniewska I, and Kaas JH. Thalamocortical connections of the parabelt auditory cortex in macaque monkeys. *J Comp Neurol* 400: 271–286, 1998b.

Hackett TA, Stepniewska I, and Kaas JH. Callosal connections of the parabelt auditory cortex in macaque monkeys. *Eur J Neurosci* 11: 856–866, 1999.

Hall DA, Johnsrude IS, Haggard MP, Palmer AR, Akeroyd MA, and Summerfield AQ. Spectral and temporal processing in human auditory cortex. *Cereb Cortex* 12: 140–149, 2002.

Howard MA, Volkov IO, Abbas PJ, Damasio H, Ollendieck MC, and Granner MA. A chronic microelectrode investigation of the tonotopic organization of human auditory cortex. *Brain Res* 724: 260–264, 1996a.

Howard MA, Volkov IO, Granner MA, Damasio HM, Ollendieck MC, and Bakken HE. A hybrid clinical-research depth electrode for acute and chronic in vivo microelectrode recording of human brain neurons [Technical note]. *J Neurosurg* 84: 129–132, 1996b.

Howard MA, Volkov IO, Mirsky R, Garell PC, Noh MD, Granner M, Damasio H, Steinschneider M, Reale RA, Hind JE, and Brugge JF. Auditory cortex on the posterior superior temporal gyrus of human cerebral cortex. *J Comp Neurol* 416: 76–92, 2000.

Imbert M, Bignall KE, and Buser P. Neocortical interconnections in the cat. *J Neurophysiol* 29: 382–395, 1966.

Imig TJ, Ruggero MA, Kitzes LM, Javel E, and Brugge JF. Organization of auditory cortex in the owl monkey (*Aotus trivirgatus*). *J Comp Neurol* 171: 111–128, 1977.

Kaas JH and Hackett TA. Subdivisions of auditory cortex and levels of processing in primates. *Audiol Neurootol* 3: 73–85, 1998.

Kaas JH, Hackett TA, and Tramo MJ. Auditory processing in primate cerebral cortex. *Curr Opin Neurobiol* 9: 164–170, 1999.

Kitzes LM and Doherty D. Influence of callosal activity on units in the auditory cortex of ferret (*Mustela putorius*). *J Neurophysiol* 71: 1740–1751, 1994.

Liegeois-Chauvel C, Musolino A, and Chauvel P. Localization of the primary auditory area in man. *Brain* 114: 139–151, 1991.

Merzenich MM and Brugge JF. Representation of the cochlear partition of the superior temporal plane of the macaque monkey. *Brain Res* 50: 275–296, 1973.

Mesulam MM and Pandya DN. The projections of the medial geniculate complex within the Sylvian fissure of the rhesus monkey. *Brain Res* 60: 315–333, 1973.

Mitani A and Shimokouchi M. Neuronal connections in the primary auditory cortex: an electrophysiological study in the cat. *J Comp Neurol* 235: 417–429, 1985.

Mitani A, Shimokouchi M, and Nomura S. Effects of stimulation of the primary auditory cortex upon colliculogeniculate neurons in the inferior colliculus of the cat. *Neurosci Lett* 42: 185–189, 1983.

Mitzdorf U. Current source-density method and application in cat cerebral cortex: investigation of evoked potential and EEG phenomena. *Physiol Rev* 65: 37–100, 1985.

Mitzdorf U. Physiological sources of evoked potentials. *Electroencephalogr Clin Neurophysiol Suppl* 42: 47–57, 1991.

Mitzdorf U. Properties of cortical generators of event-related potentials. *Pharmacopsychiatry* 27: 49–51, 1994.

Mitzdorf U and Singer W. Prominent excitatory pathways in the cat visual cortex (A 17 and A 18): a current source density analysis of electrically evoked potentials. *Exp Brain Res* 33: 371–394, 1978.

Morel A, Garraghty PE, and Kaas JH. Tonotopic organization, architectonic fields, and connections of auditory cortex in macaque monkeys. *J Comp Neurol* 335: 437–459, 1993.

Morel A and Kaas JH. Subdivisions and connections of auditory cortex in owl monkeys. *J Comp Neurol* 318: 27–63, 1992.

Morosan P, Rademacher J, Schleicher A, Amunts K, Schormann T, and Zilles K. Human primary auditory cortex: cytoarchitectonic subdivisions and mapping into a spatial reference system. *Neuroimage* 13: 684–701, 2001.

Ojemann GA and Engel JJr. Acute and chronic intracranial recording and stimulation. In: *Surgical Treatment of Epilepsies*, edited by Engel J Jr. New York: Raven Press, 1986, p. 263–288.

Pandya DN, Hallett M, and Kmukherjee SK. Intra- and interhemispheric connections of the neocortical auditory system in the rhesus monkey. *Brain Res* 14: 49–65, 1969.

Pandya DN, Karol EA, and Lele PP. The distribution of the anterior commissure in the squirrel monkey. *Brain Res* 49: 177–180, 1973.

Pandya DN, Rosene DL, and Doolittle AM. Corticothalamic connections of auditory-related areas of the temporal lobe in the rhesus monkey. *J Comp Neurol* 345: 447–471, 1994.

Pandya DN and Sanides F. Architectonic parcellation of the temporal operculum in rhesus monkey and its projection pattern. *Z Anat Entwickl-Gesch* 139: 127–161, 1973.

Rademacher J, Caviness V, Steinmetz H, and Galaburda A. Topographical variation of the human primary cortices; implications for neuroimaging, brain mapping and neurobiology. *Cereb Cortex* 3: 313–329, 1993.

Ranck JB. Which elements are excited in electrical stimulation of mammalian central nervous system: a review. *Brain Res* 98: 417–440, 1975.

Rauschecker JP. Parallel processing in the auditory cortex of primates. *Audiol Neurootol* 3: 86–103, 1998.

Rauschecker JP, Tian B, and Hauser M. Processing of complex sounds in the macaque nonprimary auditory cortex. *Science* 268: 111–114, 1995.

Rauschecker JP, Tian B, Pons T, and Mishkin M. Serial and parallel processing in rhesus monkey auditory cortex. *J Comp Neurol* 382: 89–103, 1997.

Rivier F and Clarke S. Cytochrome oxidase, acetylcholinesterase, and NADPH-diaphorase staining in human supratemporal and insular cortex: evidence for multiple auditory areas. *Neuroimage* 6: 288–304, 1997.

Seltzer B and Pandya DN. Afferent cortical connections and architectonics of the superior temporal sulcus and surrounding cortex in the rhesus monkey. *Brain Res* 149: 1–24, 1978.

Steinschneider M, Tenke CE, Schroeder CE, Javitt DC, Simpson GV, Arezzo JC, and Vaughn HG. Cellular generators of the cortical auditory evoked potential initial component. *Electroencephalogr Clin Neurophysiol* 84: 196–200, 1992.

Sugar O, French JD, and Chusid JG. Corticocortical connections of the superior surface of the temporal operculum in the monkey (*Macaca mulatta*). *J Neurophysiol* 11: 175–184, 1948.

Talavage TM, Ledden PJ, Benson RR, Rosen BR, and Melcher JR. Frequency-dependent responses exhibited by multiple regions in human auditory cortex. *Hear Res* 150: 225–244, 2000.

Vaughan HG Jr and Arezzo JC. The neural basis of event-related potentials. In: *Human Event-Related Potentials*, edited by Picton TW. Amsterdam: Elsevier, 1988, p. 45–96.

Walker AE. *The Primate Thalamus.* Chicago, IL: University of Chicago Press, 1938.

Wallace MN, Johnston PW, and Palmer AR. Histochemical identification of cortical areas in the auditory region of the human brain. *Exp Brain Res* 143: 499–508, 2002.

Ward AA, Peden JK, and Sugar O. Cortico-cortical connections in the monkey with special reference to area 6. *J Neurophysiol* 9: 353–462, 1946.

Waxman SG and Swadlow HA. The conduction properties of axons in central white matter. *Prog Neurobiol* 8: 297–324, 1977.

Wessinger CM, VanMeter J, Tian B, Van Lare J, Pekar J, and Rauschecker JP. Hierarchical organization of the human auditory cortex revealed by functional magnetic resonance imaging. *J Cogn Neurosci* 13: 1–7, 2001.

Wilson CL, Isokawa M, Babb TL, and Crandall PH. Functional connections in the human temporal lobe. I. Analysis of limbic system pathways using neuronal responses evoked by electrical stimulation. *Exp Brain Res* 82: 279–292, 1990.

Woolsey CN. Tonotopic organization of the auditory cortex. In: *Physiology of the Auditory System: A Workshop*, edited by Sachs MB. Baltimore, MD: National Educational Consultants, 1971, p. 271–282.

Yeomans JS. *Principles of Brain Stimulation.* Oxford, UK: Oxford Univ. Press, 1990.